Detection of Fe 3d electronic states in the valence band and magnetic properties of Fe-doped ZnO film*

Chen Tie-Xin(陈铁锌)[a], Cao Liang(曹 亮)[a], Zhang Wang(张 旺)[a], Han Yu-Yan(韩玉岩)[a], Zheng Zhi-Yuan(郑志远)[a], Xu Fa-Qiang(徐法强)[a]†, Ibrahim Kurash(奎热西)[b], Qian Hai-Jie(钱海杰)[b], and Wang Jia-Ou(王嘉鸥)[b]

[a] *National Synchrotron Radiation Laboratory, University of Science and Technology of China, Hefei* 230026, *China*
[b] *Beijing Synchrotron Radiation Facility, Institute of High Energy Physics, Chinese Academy of Sciences, Beijing* 100049, *China*

(Received 9 May 2012; revised manuscript received 22 August 2012)

Fe-doped ZnO film has been grown by laser molecular beam epitaxy (L-MBE) and structurally characterized by X-ray diffraction (XRD) and scanning electron microscopy (SEM), all of which reveal the high quality of the film. No secondary phase was detected. Resonant photoemission spectroscopy (RPES) with photon energies around the Fe 2p–3d absorption edge is performed to detect the electronic structure in the valence band. A strong resonant effect at a photon energy of 710 eV is observed. Fe^{3+} is the only valence state of Fe ions in the film and the Fe 3d electronic states are concentrated at binding energies of about 3.8 eV and 7 eV∼8 eV. There are no electronic states related to Fe near the Fermi level. Magnetic measurements reveal a typical superparamagnetic property at room temperature. The absence of electronic states related to Fe near the Fermi level and the high quality of the film, with few defects, provide little support to ferromagnetism.

Keywords: Fe-doped ZnO, laser molecular beam epitaxy, resonant photoemission spectroscopy, superparamagnetism

PACS: 61.05.cp, 68.37.Hk, 73.61.Ga, 75.50.Pp **DOI:** 10.1088/1674-1056/22/2/026101

1. Introduction

Recently, great progress has been made in diluted magnetic semiconductors (DMS), which incorporate transition-metal (TM) magnetic ions in semiconductor material, bringing up the development of spintronic electron theory,[1] which combines the two important characteristics of charges and spins. The great potential application of DMS in making spintronic devices has drawn more and more people's attention regarding data-processing speed, nonvolatility, and higher integration densities.[2,3] It will probably turn out to be a very promising technology in the future, since the concept of spintronic device has come into being on the basis of DMS, which exhibits ferromagnetism at room temperature. Among many kinds of semiconductor materials, ZnO is the most widely used base material. ZnO has a prominent wide band gap ($E_g = 3.37$ eV) and a large exciton binding energy (60 meV), which can lead to a lasing action above room temperature based on exciton recombination.[4] Also, it can easily be doped with TM, and there are many growth techniques to prepare high-quality ZnO films. Ohno[5] first developed the concept of DMS and stimulated the tendency to study DMS. With the Zener model, Dietl *et al.*[6] predicted that Mn-doped ZnO and GaN are the only semiconductor materials that will reveal ferromagnetism at room temperature. Sharma *et al.*[7] demonstrated this prediction by experimentally showing that Mn-doped ZnO could be ferromagnetic above room temperature with the average magnetic moment of 0.16 μ_B/Mn. More theoretical works have also appeared in recent years. Density functional calculations with local spin density approximation (LSDA) and LSDA+U methods have been carried out to study the electronic structure of TM-doped ZnO.[8–10]

Although the origin of ferromagnetism has been widely discussed to unravel its essence, it is still a controversial problem for TM-doped ZnO. A carrier-mediated mechanism has frequently been proposed, which suggests that free carriers mediate the exchange interaction.[11] In addition, the mechanism of bound magnetic polarons (BMP) has been discussed.[12–14] Dietl *et al.*[6] revealed strong coupling between valence band holes and localized spins in TM-doped ZnO. Peng *et al.*[15] showed that ZnO with acceptors displays an enhancement of hole-induced ferromagnetism in terms of the band coupling model. Karmakar *et al.*[16] demonstrated that in Fe-doped ZnO nanoparticles the presence of Zn vacancies can stabilize ferromagnetism by altering part of Fe^{2+} ions into Fe^{3+} ions. Furthermore, clusters or hidden ferromagnetic secondary phases can also induce ferromagnetism in DMS.[17] In sum, there is no consistent agreement about the origin of ferromagnetism in DMS. It is necessary to verify the roles of both intrinsic and extrinsic factors in the promotion of ferromagnetism.

In our experiment, Fe-doped ZnO film has been grown by laser molecular beam epitaxy (L-MBE) on a Si(111) substrate. The property of Fe ions regarding both valence state

*Project supported by the National Natural Science Foundation of China (Grant Nos. 10775126 and 10975138).
†Corresponding author. E-mail: fqxu@ustc.edu.cn
© 2013 Chinese Physical Society and IOP Publishing Ltd

and distribution of electronic states determines the complexity of magnetic interaction. X-ray diffraction (XRD) and scanning electron microscopy (SEM) are used to detect the structure and morphology. Resonant photoemission spectroscopy (RPES) and magnetic measurements have been performed to discuss the relationship between the electronic structure and magnetic property.

2. Experiment

Fe-doped ZnO film was grown on Si(111) substrate by using the L-MBE method. High purity Fe_2O_3 (4N) and ZnO (4N) powders were mixed together with a nominal ratio of 10% and sintered at 1200 °C to form the ceramic target with uniform states. The Si(111) substrate was first cleaned with acetone and ethanol, and then oxidized in boiled H_2SO_4:H_2O_2 (1:1) solution for 5 min, finally etched in the 5% HF solution for 3 min. A KrF excimer laser with a wavelength of 248 nm and a frequency of 2 Hz was used as the laser source. The distance between the target and the substrate was about 15 cm. The initial vacuum pressure in the chamber was 5×10^{-7} Pa. During the growth process, ultrahigh purity oxygen (4N) was introduced into the chamber and the pressure was maintained at 5×10^{-4} Pa to avoid O vacancies in the sample. The growth time was about 1 h. The concentration of Fe in the film was measured to be 8.8% by X-ray fluorescence spectroscopy (XRF). The film thickness is 55 nm.

X-ray absorption spectroscopy (XAS) and resonant photoemission spectroscopy (RPES) were carried out on the beamline of the Beijing Synchrotron Radiation Facility (BSRF) at the Institute of High Energy Physics, Chinese Academy of Sciences. A VSW HA150 electron energy analyzer was used for the studies. The energy resolution power, $E/\Delta E$, was $\sim$ 1500. The XAS measurement was performed at the Fe L-edge in a total electron yield mode with an incident angle of 45° with respect to the sample surface. The RPES measurements were performed in the energy distribution curve (EDC) mode using the photon energies according to the XAS measurement. All spectra were normalized by the incident beam current. To confirm the crystal structure and the quality of the film, X-ray diffraction (XRD, TTR-III) and field emission scanning microscopy (SEM, Sirion200) measurements were performed. To obtain the magnetic property of the film, magnetization (M) versus magnetic field (H) curves at 4 K and room temperature (300 K), magnetization (M) versus temperature (T) curves were measured on a superconducting quantum interference device (SQUID).

3. Results and discussion

Figure 1 illustrates the XRD patterns of the mixed ceramic target and the Fe-doped ZnO film. It is shown in Fig. 1(a) that the indexed peaks come from the typical XRD pattern of powder ZnO in the ceramic target and the tiny peaks indicated by the arrows correspond to the zinc ferrite ($ZnFe_2O_4$) phase. After the mixed powder was sintered at high temperature via the reaction of ZnO and Fe_2O_3, the

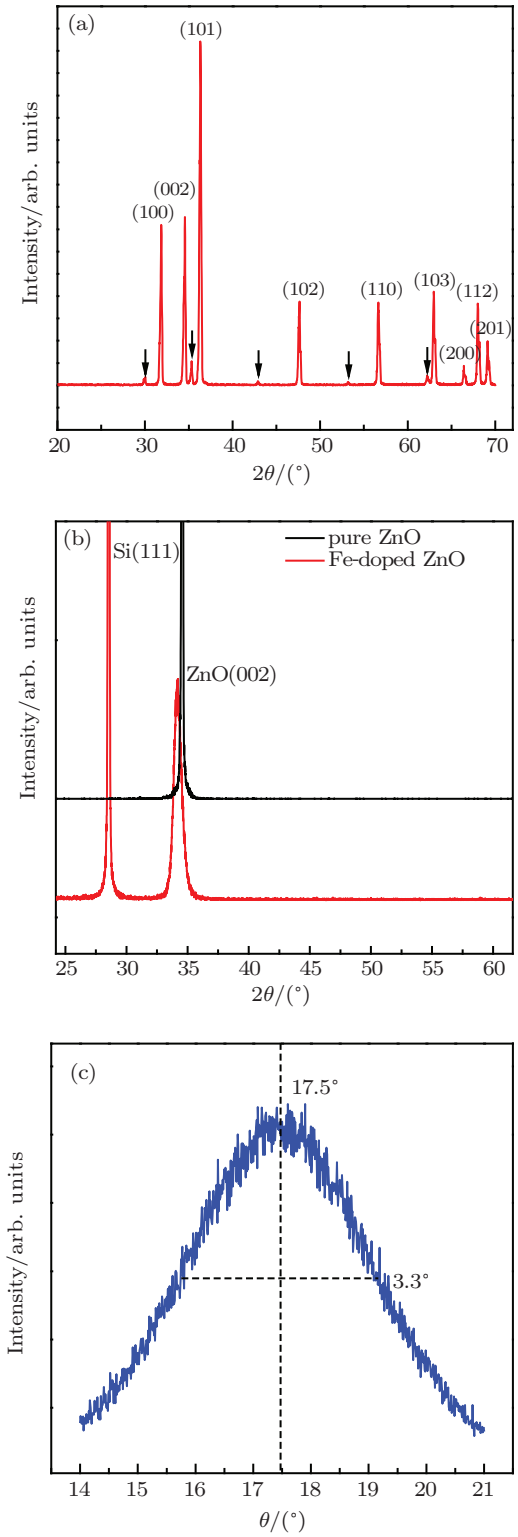


Fig. 1. (color online) Structural measurements of the Fe-doped ZnO film: (a) XRD pattern of the ceramic target; (b) XRD pattern of pure ZnO and the film grown by L-MBE. There is a distinct movement for the ZnO(002) peak; (c) rocking curve of the film.

secondary $ZnFe_2O_4$ phase was produced. Bulk $ZnFe_2O_4$ has a spinel structure with paramagnetic properties, in which Zn atoms are located at tetrahedral sites and Fe atoms are located at octahedral sites.[18] In Fig. 1(b), however, after growth by L-MBE, only one peak at about 34.2° is observed, indicating that the Fe-doped ZnO film grows with a *c*-axis preferred orientation. Under the detective sensitivity of XRD scanning, there is no secondary phase or clusters formed in the film, which differs from the components in the ceramic target. It is confirmed that Fe ions have dispersed uniformly into the crystal lattice of ZnO, but it cannot be simply concluded that Fe ions substitute for Zn ions in the film. In Fig. 1(b), compared with the pure ZnO, the ZnO(002) peak position of the Fe-doped ZnO film has moved 0.3° to a lower level, which means the *c*-axis lattice constant increases slightly after Fe doping. This fact is inconsistent with the assertion that Fe ions substitute for Zn ions and with the existence of vacancies in the film, because the lattice constant would decrease with the substitution of Fe in ZnO. Instead, the Fe ions may occupy the interstitial octahedral sites in the film. In Fig. 1(c), the rocking curve with respect to the ZnO(002) peak shows that the full width at half maximum (FWHM) is about 3.3°, indicating high crystal quality of the film. In Fig. 2, the SEM image shows a relatively smooth and compact surface without many grains or other structures related to impurities. Therefore, the existence of Fe ions in the system is homogeneous.

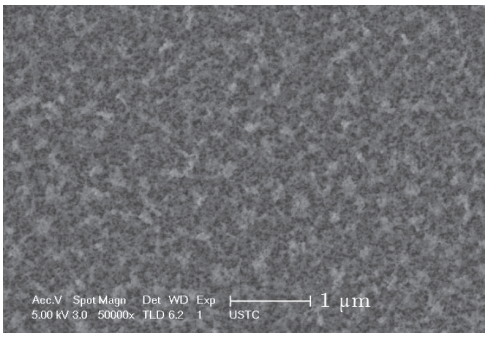


Fig. 2. SEM image of the Fe-doped ZnO film grown by L-MBE.

RPES measurement is implemented to detect the electronic structure of the Fe-doped ZnO film. The concentration of transition metal in DMS is low and the information about Fe 3d electronic states in the valence band is so weak that it is difficult to detect. Therefore, RPES is an effective instrument to study the electronic states in DMS. There are two interesting processes[19] in 2p–3d RPES for transition metal: direct photoemission process and Coster–Kronig Auger decay associated with absorption. The formula of this process can be written as

$$2p^63d^6 + h\nu \rightarrow 2p^53d^7 \rightarrow 2p^63d^5 + e(+2p^63d^6L + 2p^63d^7L^2\cdots),$$

where *L* denotes a ligand hole hybridized with 3d in the final states. In our system, if the photon energy is equal to the Fe 2p absorption edge, there is an enhancement resonant effect adding to the intensity of Fe 3d direct photoemission. Therefore, the Fe 3d electronic states can be detected in this way.

Fe *L*-edge XAS spectra measured at photon energy of 698 eV to 730 eV is shown in Fig. 3. The main peak is at photon energy of 710 eV corresponding to the Fe^{3+} ions' absorption edge, indicating that the dominant Fe valence state in the film is Fe^{3+} ions. In order to search for the Fe 3d electronic states in the valence band, RPES have been measured with photon energies from 698 eV to 730 eV according to Fe *L*-edge XAS spectra. In Fig. 4, a significant enhancement effect is observed when photon energy is at 710 eV and 723 eV, which is consistent with the absorption peaks in Fe *L*-edge XAS. There are three peaks available in the spectra, which is in agreement with the valence band of pure ZnO. The peaks at about 10.7 eV, 4.5 eV, and 7.5 eV are attributed to Zn 3d, O 2p electronic states, and hybridization states of O 2p and Zn 4s, respectively.[20]

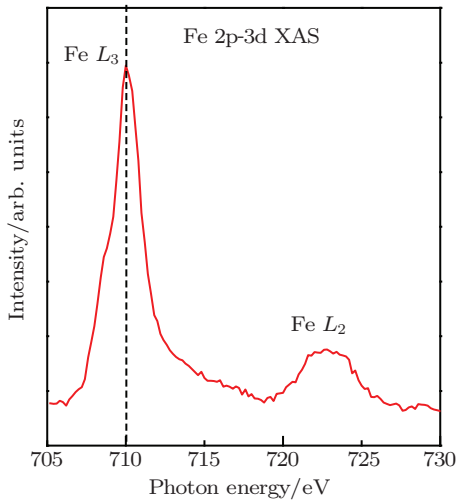


Fig. 3. (color online) Fe $L_{2,3}$ XAS of the Fe-doped ZnO film. The main peak at 710 eV, denoted by the dash line, corresponds to the absorption edge of Fe^{3+} ions.

In Fig. 5(a), photon energies of 710 eV and 708 eV correspond to Fe^{3+} and Fe^{2+} absorption peaks, respectively. All the spectra are normalized with respect to Zn 3d peak intensity. Basically, the electronic states near the Fermi level have a close relationship with the electronic and magnetic properties of DMS, in which it is not unusual to discover the electronic states related to the magnetic ions.[21,22] In order to distinguish and have a deep insight into the Fe 3d electronic states in the valence band, the difference spectrum obtained by subtracting off-resonant spectrum (704 eV) from on-resonant spectrum (710 eV and 708 eV) are shown in Fig. 5(b). It is observed that the main locations of Fe^{3+} 3d electronic states appear at the binding energy of about 3.8 eV and 7 eV∼8 eV. There is no confirmed evidence of the existence of Fe^{2+} ions in our

sample. In the band gap from the Fermi level to about 2 eV, no enhancement effect associated with Fe 3d electronic states is observed, indicating that there are no electronic states related to Fe ions near the Fermi level.

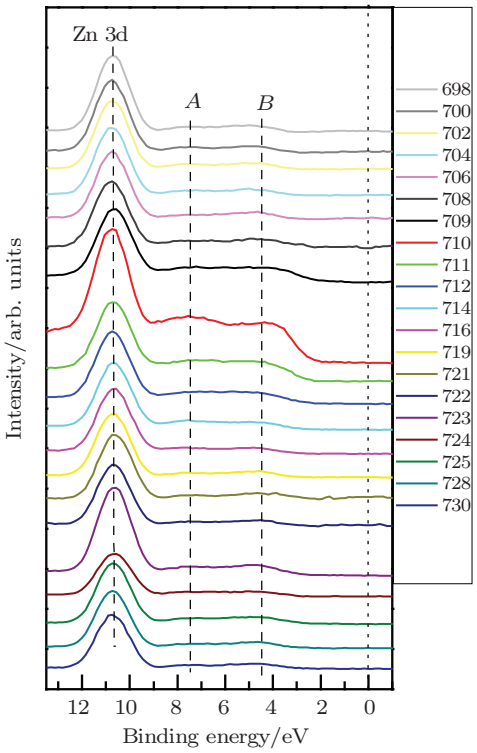


Fig. 4. (color online) RPES spectra of the Fe-doped ZnO film. The peak at 10.7 eV corresponds to Zn 3d electronic states. Peak *A* comes from hybridization of O 2p and Zn 4s, peak *B* comes from O 2p electronic states. The dotted line is the Fermi level.

In Fig. 6(a), the magnetization (M) versus magnetic field (H) curves are measured at both low temperature (4 K) and room temperature (300 K). No obvious hysteresis loops were detected, indicating that the sample is not ferromagnetic. In Fig. 6(b), magnetization (M) versus temperature (T) curves are measured with a magnetic field of 1000 Oe (1 Oe=79.5775 A/m). It is clear that the field cooled (FC) and zero-field cooled (ZFC) curves exhibit irreversibility due to the prominent cusp indicated by the arrow. This feature comes from the typical blocking process of superparamagnetic nanoparticles, in which the contribution of paramagnetic interaction decreases significantly.[23] The magnetic measurements suggest a superparamagnetic property at room temperature with an extremely high saturation magnetization in the Fe-doped ZnO film.

Combined with our earlier structural analysis, it is confirmed that its clusters are unlikely to form and Fe^{3+} ions are located uniformly throughout the system. The magnetic property is an intrinsic property of the film. The distribution of Fe^{3+} ions in the crystal lattice probably has the same pattern as in $ZnFe_2O_4$.[24] The XRD results provide some evidence about this inference. Yao *et al.*[25] have shown that in synthetic $ZnFe_2O_4$ nanocrystals the redistribution of Fe ions between tetrahedral sites and octahedral sites can lead to superparamagnetism at room temperature. This provides us with

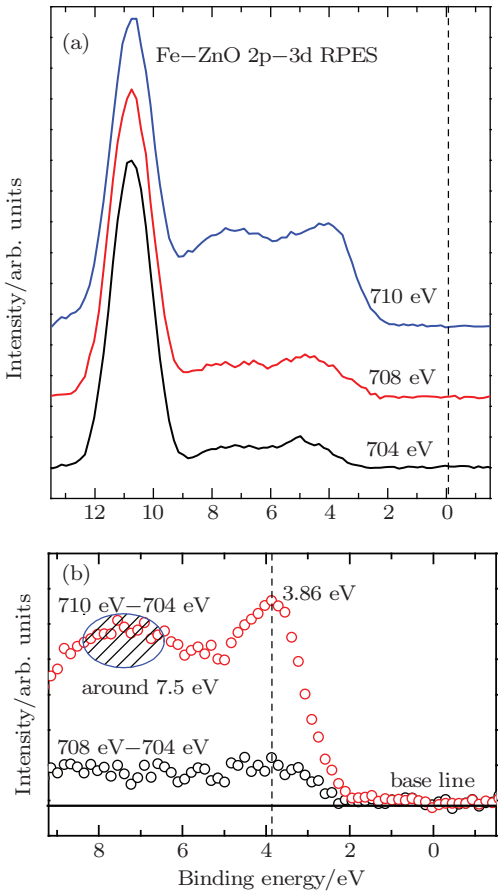


Fig. 5. (color online) Fe 2p–3d RPES of the Fe-doped ZnO film (a) and the 710 eV–704 eV, 708 eV–704 eV difference spectra (b).

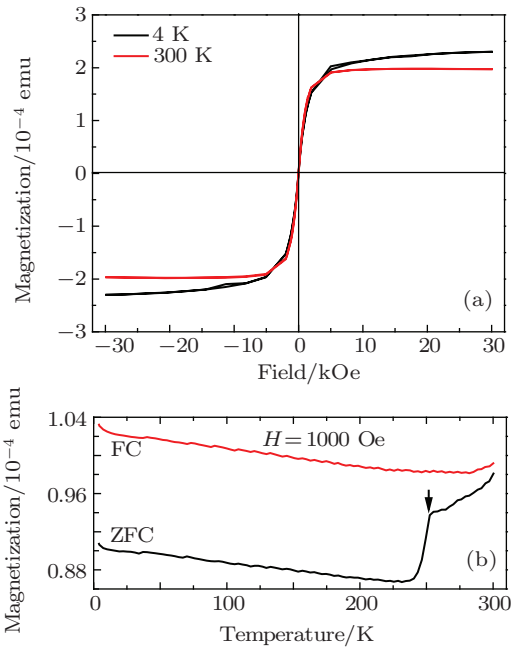


Fig. 6. (color online) Magnetization (M) versus magnetic field (H) curve of the Fe-doped ZnO film, measured at 4 K and 300 K (a) and magnetization (M) versus temperature (T) curves with the magnetic field of 1000 Oe (b). The arrow indicates the cusp observed in the zero-field cooled (ZFC) curve.

a comprehensive understanding about the magnetic properties in our sample. When Fe atoms are doped into ZnO, the electronic structure is deeply influenced by the charge effect or ligand environment,[22] which causes the Fe 3d electronic states to change under various conditions. In our system, the high quality of the film and the lack of Fe^{2+} ions as well as the electronic states related to Fe ions near the Fermi level clearly make little contribution to ferromagnetism.

4. Conclusion

Fe-doped ZnO thin film is grown by L-MBE with perfect *c*-axis orientation. Structural analysis shows the high quality of the film and less likelihood of the existence of secondary phase. Fe ions spread homogeneously in the crystal lattice and the valence state of Fe ions is Fe^{3+}. Obvious resonant effect is observed in Fe 2p–3d RPES. Fe 3d electronic states are located at binding energies of about 3.8 eV and 7 eV∼8 eV. There are no electronic states related to Fe ions observed near the Fermi level. Magnetic measurements suggest a superparamagnetic property with high saturation magnetization at room temperature. In the Fe-doped ZnO system, the high crystal quality and the lack of Fe^{2+} ions do not facilitate ferromagnetism. Electronic states near the Fermi level and the presence of defects may play important roles in the formation of ferromagnetism.

References

[1] Dash S P, Sharma S, Patel R S, de Jong M P and Jansen R 2009 *Nature* **462** 491
[2] Prinz G A 1998 *Science* **282** 1660
[3] Lou X H, Adelmann C, Crooker S A, Garlid E S, Zhang J, Reddy K S M, Flexner S D, Palmstrom C J and Crowell P A 2007 *Nat. Phys.* **3** 197
[4] Ozgur U, Alivov Y I, Liu C, Teke A, Reshchikov M A, Dogan S, Avrutin V, Cho S J and Morkoc H 2005 *J. Appl. Phys.* **98** 041301
[5] Ohno H 1998 *Science* **281** 951
[6] Dietl T, Ohno H, Matsukura F, Cibert J and Ferrand D 2000 *Science* **287** 1019
[7] Sharma P, Gupta A, Rao K V, Owens F J, Sharma R, Ahuja R, Guillen J M O, Johansson B and Gehring G A 2003 *Nat. Mater.* **2** 673
[8] Debernardia A and Fanciulli M 2007 *Appl. Phys. Lett.* **90** 212510
[9] Ganguli N, Dasgupta I and Sanyal B 2009 *Appl. Phys. Lett.* **94** 192503
[10] Jug K and Tikhomirov V A 2009 *J. Phys. Chem.* A **113** 11651
[11] He Y, Sharma P, Biswas K, Liu E Z, Ohtsu N, Inoue A, Inada Y, Nomura M, Tse J S, Yin S and Jiang J Z 2008 *Phys. Rev.* B **78** 155202
[12] Kaminski A and Das Sarma S 2002 *Phys. Rev. Lett.* **88** 247202
[13] Durst Adam C, Bhatt R N and Wolff P A 2002 *Phys. Rev.* B **65** 235205
[14] Coey J M D, Venkatesan M and Fitzgerald C B 2005 *Nat. Mater.* **4** 173
[15] Peng H W, Xiang H J, Wei S H, Li S S, Xia J B and Li J B 2009 *Phys. Rev. Lett.* **102** 017201
[16] Karmakar D, Mandal S K, Kadam R M, Paulose P L, Rajarajan A K, Nath T K, Das A K, Dasgupta I and Das G P 2007 *Phys. Rev.* B **75** 144404
[17] Kaspar T C, Droubay T, Heald S M, Engelhard M H, Nachimuthu P and Chambers S A 2008 *Phys. Rev.* B **77** 201303
[18] Jeyadevan B, Tohji K and Nakatsuka K 1994 *J. Appl. Phys.* **76** 6325
[19] Kamata A, Noguchi K, Suzuki K, Tezuka H, Kashiwakura T, Ohno Y and Nakai S 1997 *J. Phys. Soc. Jpn.* **66** 401
[20] Ozawa K, Oba Y, Edamoto K, Higashiguchi M, Miura Y, Tanaka K, Shimada K, Namatame H and Taniguchi M 2009 *Phys. Rev.* B **79** 075314
[21] Kataoka T, Kobayashi M, Sakamoto Y, Song G S, Fujimori A, Chang F H, Lin H J, Huang D J, Chen C T, Ohkochi T, Takeda Y, Okane T, Saitoh Y, Yamagami H, Tanaka A, Mandal S K, Nath T K, Karmakar D and Dasgupta I 2010 *J. Appl. Phys.* **107** 033718
[22] Leonov I, Yaresko A N, Antonov V N and Anisimov V I 2006 *Phys. Rev.* B **74** 165117
[23] Martínez B, Sandiumenge F, Balcells L, Arbiol J, Sibieude F and Monty C 2005 *Phys. Rev.* B **72** 165202
[24] Pan F, Guo Y, Cheng F F, Fa T and Yao S D 2011 *Chin. Phys.* B **20** 127501
[25] Yao C W, Zeng Q S, Goya G F, Torres T, Liu J F, Wu H P, Ge M Y, Zeng Y W, Wang Y W and Jiang J Z 2007 *J. Phys. Chem.* C **111** 12274